Available online at www.sciencedirect.com

SciVerse ScienceDirect

Ceramics International 38 (2012) 3955–3961

CERAMICS INTERNATIONAL

www.elsevier.com/locate/ceramint

Assessment of thermochemically stable apatite $La_{10}(SiO_4)_6O_3$ as electrolyte for solid oxide fuel cells

Yu-Lin Kuo *, Yun-Yuan Liang

Department of Mechanical Engineering, National Taiwan University of Science and Technology, 43, Keelung Road, Section 4, Taipei 106, Taiwan

Received 8 December 2011; received in revised form 19 January 2012; accepted 20 January 2012
Available online 27 January 2012

Abstract

Apatite-type lanthanum silicate with a formula of $La_{10}(SiO_4)_6O_3$ is a potential candidate electrolyte for SOFC system because of its high ionic conductivity and low activation energy. Pure $La_{10}(SiO_4)_6O_3$ powder was prepared by solid state reaction and using a suitable thermal pretreatment (1000 °C/5 h) of the as-purchased La_2O_3 powder. Materials characterization, thermal behaviors, and electrical properties of $La_{10}(SiO_4)_6O_3$ samples were investigated by X-ray diffraction (XRD), scanning electron microscopy (SEM), thermogravimetric analysis (TGA) and two-point probe DC conductivity. A pure $La_{10}(SiO_4)_6O_3$ pellet was prepared at the sintering process of 1600 °C and 2.5 h with a high relative sintered density of 96.91%. The existence of secondary phases in $La_{10}(SiO_4)_6O_3$ pellet resulted in a lower conductivity than that of pure $La_{10}(SiO_4)_6O_3$ pellet. Eight-hour reduction-resistant stability tests under reducing atmosphere at the elevated temperature of pure $La_{10}(SiO_4)_6O_3$ prepared in this study shows a good thermochemical stability as compared to the well-developed 8 mol% Y_2O_3 stabilized ZrO_2 (8YSZ).

Keywords: D. Apatite; Lanthanum silicate; $La_{10}(SiO_4)_6O_3$; Solid oxide fuel cells (SOFCs); Thermochemical stability

1. Introduction

8YSZ is the most mature material to be an electrolyte in traditional solid oxide fuel cells (SOFCs). Owing to its low ionic conductivity, however, SOFC systems usually operated at elevated temperatures (800–1000 °C) for a higher efficiency of power generators. Thus, several issues such as thermal mismatch between ceramic components and coking problems etc. should be considered carefully due to its high operation temperature [1]. In order to reduce the operation temperature of SOFCs from 800 °C to 500 °C while maintaining the higher power generation efficiency, the main current researches have been focused on the developments of preparing a thin-film electrolyte (<10 μm) [2–4] and new electrolyte materials with higher conductivity [5–8] to decrease the resistance of cells.

Rare earth silicates with an apatite-type structure were discovered as a novel oxide-ion conductor for its exceptional ionic conductivity of oxygen ions, lower activation energy and excellent stability [8–10]. Rather than the electrolytes with fluorite (e.g. doped ZrO_2, CeO_2) and perovskite (e.g. doped $LaGaO_3$) related structures with high symmetric structures, the apatite silicates with a high ionic conduction are believed to migrate via an interstitial pathway mechanism. Excess oxide ions in the apatite silicates can be introduced in the structure and enhance the oxide-ion migration in the conduction channel along the *c*-axis, which is in contrast to the oxide ion vacancy mechanism in perovskite and fluorite-type oxide ion conductors [8–10].

Nakayama et al. have firstly declared the ionic conductivities of lanthanoid silicate of the $Ln_{10}(SiO_4)_6O_3$ (Ln: La, Nd, Sm, Gd, Dy, Y, Ho, Er and Yb) solid solution series [11,12]. Among these lanthanoid silicate series, doped lanthanum silicate, $La_{10}(SiO_4)_6O_3$, is believed to be a good candidate electrolyte for SOFC use, because of its higher ionic conductivity at lower temperatures (500–800 °C). According to their results of the hexagonal structure of the $La_{10}(SiO_4)_6O_3$ (space group: $P6_3/rn$) ceramics determined by the Rietveld method, a three-dimensional (3D) network structure is established by inter-connection of the tetrahedral-site SiO_4 and the octahedral-site LaO. Besides, they also referred that the mobile oxygen ions located at the 2a site are surrounded by lanthanum ions at the 6h positions [11,12].

* Corresponding author at: No. 43, Section 4, Keelung Road, Taipei 10607, Taiwan. Tel.: +886 2 27376784; fax: +886 2 27376460.
E-mail address: ylkuo@mail.ntust.edu.tw (Y.-L. Kuo).

0272-8842/$36.00
doi:10.1016/j.ceramint.2012.01.049

For the preparation of lanthanum silicate from La_2O_3 and SiO_2 as starting materials by solid state reaction, either La_2SiO_5 or $La_2Si_2O_7$ with lower ionic conductivity is easily formed as secondary phase, which might be due to the inevitable absorption of La_2O_3 by H_2O and CO_2 from the ambient atmosphere. Thus, Béchade et al. proposed a new faster and lower temperature method for preparing pure apatite-type lanthanum silicate from a solid-state method by using an appropriate thermal treatment of the starting mixture [13]. Besides, Nakao et al. have referred a single solid oxide fuel cell with a sandwiched structure of $Pt/La_{10}(SiO_4)_6O_3/Pt$ under a presence of CO_2 in a hydrogen fuel gas [14]. In the chemical stability test of their fabricated single-cell system, the cell voltage under a constant current density was stable during the operation for over 100 h.

In this study, the material investigated is strictly focused on preparation and characterization of $La_{10}(SiO_4)_6O_3$ by solid state reaction and using a suitable thermal pretreatment (1000 °C for 5 h) of the as-purchased La_2O_3 powder. XRD and SEM were used to examine the microstructural morphology, crystal structure, and surface porosity of the sintered pellets. TGA/DTA was used for analyzing the thermal behavior of the calcination process for different La_2O_3/SiO_2 powder under nitrogen atmosphere. Archimedes method was applied to measure the relative densities of the samples. The thermochemical stability of $La_{10}(SiO_4)_6O_3$ powder at temperatures of 500–800 °C under reducing atmosphere was carried out by TGA as compared to the common electrolytes 8YSZ, Bi_2O_3 and GDC10 (Gadolinium Doped Ceria, $Ce_{0.9}Gd_{0.1}O_{1.95}$).

2. Experimental

La_2O_3 powder (99.99%, Alfa Asear, USA) and SiO_2 powder (99.9%, Alfa Aesar, USA) were used to prepare apatite-type $La_{10}(SiO_4)_6O_3$ samples by solid state reaction process. The flowchart of the experimental steps is shown in Fig. 1. In order to determine the appropriate stoichiometry of $La_{10}(SiO_4)_6O_3$ powder, the thermal pretreatment of La_2O_3 powder under 1000 °C for 5 h was firstly performed, which could eliminate the lanthanum hydroxide ($La(OH)_3$) or lanthanum hydroxycarbonates ($La_2(OH)_{6-2x}(CO_3)_x$) due to the exposure of La_2O_3 powder to the atmosphere. A stoichiometric ratio (5:6) of thermally pretreated La_2O_3 powder and as-purchased SiO_2 powder were added in ethyl alcohol and then physically mixed and grounded at 380 rpm for 1 h by high energy ball milling in a planetary ball mill (Model PM100, Retsch, GmbH, Germany). The obtained mixture slurry was dried at a vacuum evaporator at 40 °C and subsequently calcined at a heating rate of 10 °C/min using a programmable cube furnace in air at 1200 °C for 10 h to obtain the stoichiometric reaction:

$$5La_2O_3 + 6SiO_2 \rightarrow La_{10}(SiO_4)_6O_3 \quad (1)$$

The calcined powder was uniaxially pressed at a pressure of 100 MPa to form a circular pellet of 15 mm in diameter. The pellets were then sintered at 1550–1600 °C for different hours in air at a heating rate of 5 °C/min. A Netzsch STA 449F3

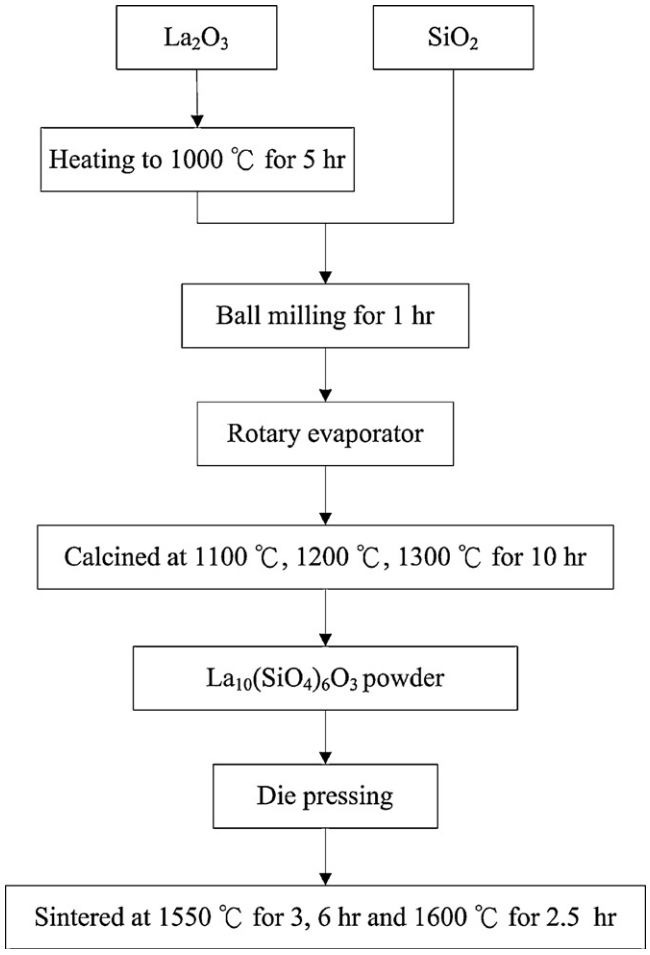

Fig. 1. Experimental flowchart of apatite-type $La_{10}(SiO_4)_6O_3$ prepared in this study.

thermogravimetric analyzer/differential thermal analysis (TGA/DTA) was used for analyzing the thermal behavior of the calcination process for different La_2O_3/SiO_2 powder under nitrogen atmosphere. Then, the calcined powder and sintered pellets were verified by the X-ray diffractometer (XRD, Bruker D2 Phaser, Cu-Kα radiation of radiation of λ = 1.5405 Å), employing a scanning rate of 0.05 deg s^{-1} in the 2θ range from 20 to 60°. Secondary electron images from SEM were used to observe the microstructural morphology and grain size of the sample. The sintered densities of $La_{10}(SiO_4)_6O_3$ pellets were then derived by the Archimedes relations. Conductivities of the sintered $La_{10}(SiO_4)_6O_3$ samples were measured at temperatures ranging from 500 °C to 800 °C. Silver electrodes of 0.1 cm diameter were secured via Ag adhesive paste, which were coated on either sides of the sample pellet and held at raised temperature for 1 h. Two-point probe DC conductivity was measured accordingly.

The thermochemical behavior of $La_{10}(SiO_4)_6O_3$ powder at temperatures of 500–800 °C under reducing atmosphere was carried out by TGA. The ramping process was firstly heating to the fixed temperature under N_2 atmosphere. Then, 20% H_2 reducing gas with a flow rate of 20 sccm was introduced to TGA chamber for the 8-h reduction-resistant stability test.

Common electrolytes of 8YSZ, Bi_2O_3 and GDC10 were also used for the comparison.

3. Results and discussion

As the previous studies of $La_{10}(SiO_4)_6O_3$ preparation, the often encountered secondary phases of La_2SiO_5 and $La_2Si_2O_7$ were observed in the case of solid state reaction process, which is resulted from the inappropriate stoichiometric reaction of La_2O_3 and SiO_2 powder during the preparation [13,15]. However, the inappropriate stoichiometric reaction is attributed to the absorption of H_2O and CO_2 of La_2O_3 from the ambient atmosphere to form $La(OH)_3$ and $La_2(OH)_{6-2x}(CO_3)_x$ during the preparation. Through the thermal pretreatment of La_2O_3 powder (t-La_2O_3) at 1000 °C for 5 h, the elimination of $La(OH)_3$ and $La_2(OH)_{6-2x}(CO_3)_x$ could be achieved [13]. In this study, the as-purchased La_2O_3 powder without the thermal pretreatment was denoted as p-La_2O_3.

Fig. 2 shows the thermal behaviors of p-La_2O_3/SiO_2 and t-La_2O_3/SiO_2 mixtures by TGA/DSC analyses. In the plots of DSC, both of these two mixtures represented four endo-transition peaks due to the possible reactions which were previous reported by Béchade et al. [13]. The peaks at 300–400 °C (peaks a and b) were attributed to the dehydration and decarbonation of $La(OH)_3$ and $La_2(OH)_{6-2x}(CO_3)_x$ to transform into LaOOH and $La_2O_2CO_3$, and both finally decomposed into La_2O_3 above 460 °C (peaks c and d). Even the thermal pretreatment of La_2O_3 powder was applied, $La(OH)_3$ and $La_2(OH)_{6-2x}(CO_3)_x$ were inevitably formed at room temperature, which were proven in Fig. 2b. Furthermore, the calcination processes applied to p-La_2O_3/SiO_2 and t-La2O3/SiO_2 mixtures were made at 1200 °C for 10 h, respectively. XRD patterns (Fig. 3(a) and (b)) show the crystalline structures of $La_{10}(SiO_4)_6O_3$ powder, indicating the existence of the secondary phases was only obtained at p-La_2O_3/SiO_2 mixture after the calcination process. Based on the possible reactions observed by Béchade et al., the smaller peaks and less weight loss of t-La_2O_3/SiO_2 mixtures at TGA/DSC plots (Fig. 2(b)) and calcined $La_{10}(SiO_4)_6O_3$ powder without secondary phases at XRD pattern (Fig. 3(b)) could evidently concluded the thermal pretreatment of La_2O_3 powder under 1000 °C for 5 h could effectively eliminate $La(OH)_3$ and $La_2(OH)_{6-2x}(CO_3)_x$ phases for the further preparation of obtaining the appropriate stoichiometry of $La_{10}(SiO_4)_6O_3$ powder.

Sintered samples of calcined $La_{10}(SiO_4)_6O_3$ powder without secondary phases at 1550 °C and 1600 °C for different time were also examined by XRD as shown in Fig. 4, which all the cases revealed a single phase $La_{10}(SiO_4)_6O_3$ with an apatite structure (JCPDs # 53-0291) and the strongest diffraction peak

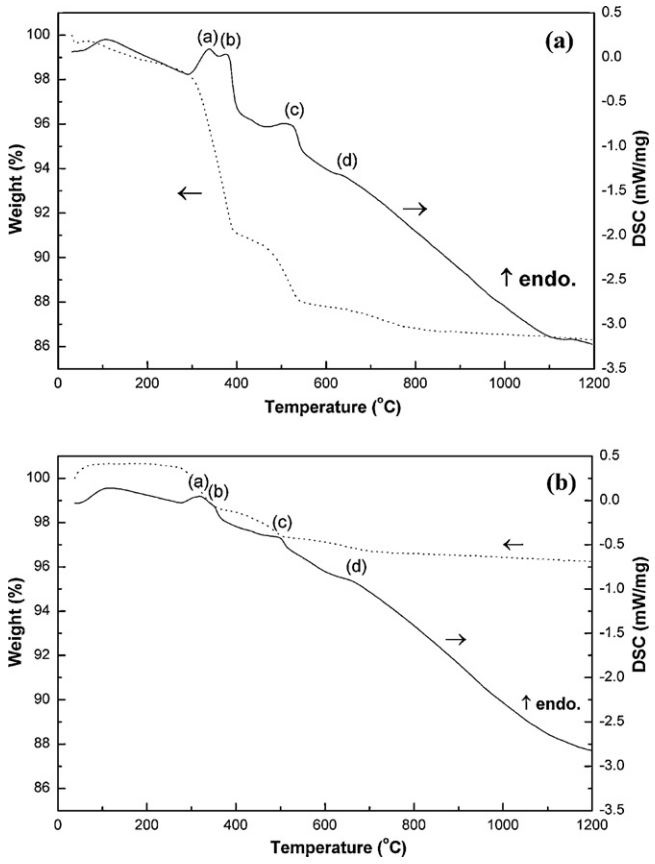

Fig. 2. TGA/DSC plots of (a) p-La_2O_3/SiO_2 and (b) t-La_2O_3/SiO_2 mixtures.

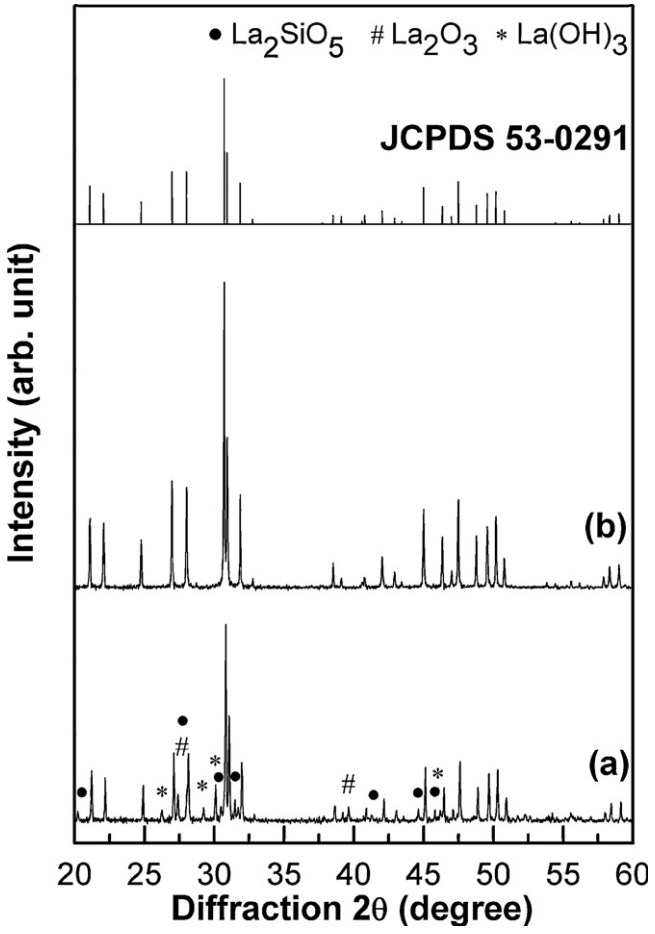

Fig. 3. XRD spectra of calcined $La_{10}(SiO_4)_6O_3$ powder prepared with the mixtures of (a) p-La_2O_3/SiO_2 and (b) t-La_2O_3/SiO_2.

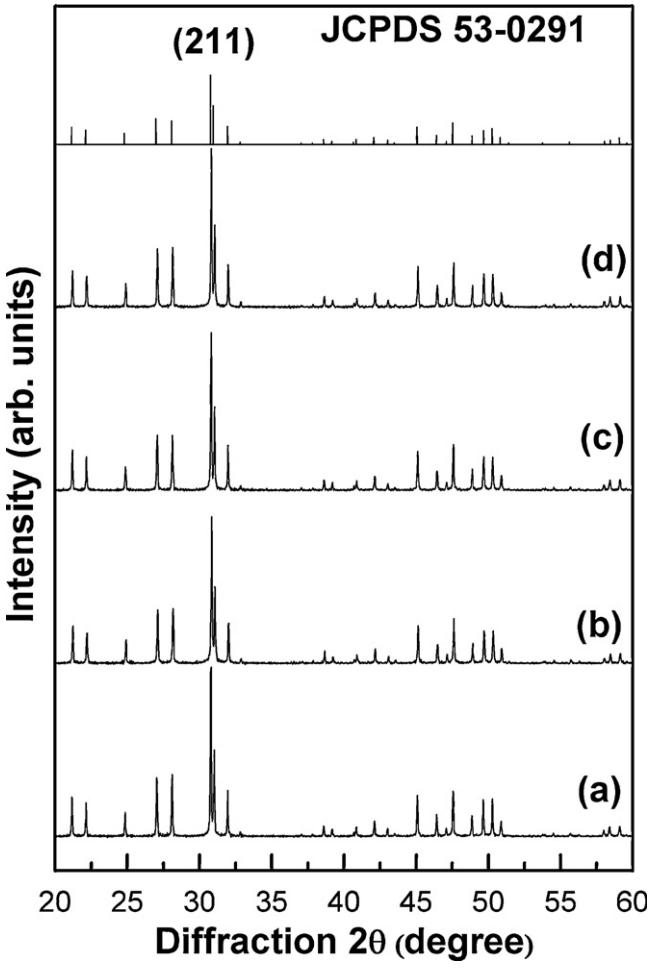

Fig. 4. XRD spectra of pure $La_{10}(SiO_4)_6O_3$ pellets sintered at different temperatures and time: (a) 1550 °C/3 h, (b)1550 °C/6 h, (c) 1550 °C/12 h, and (d) 1600 °C/2.5 h.

of (2 1 1) plane is recorded at the 2θ of 31.9°. The calculated lattice parameters of sintered $La_{10}(SiO_4)_6O_3$ pellets ($a = b = 9.707$ Å and $c = 7.174$ Å) were in a good agreement with previous literatures [11–13] and the corresponding Joint Commission on Powder Diffraction Standards (JCPDs) file card (JCPDs # 53-0291).

The densities of the samples were separately measured according to Archimedes method. The relative densities of the samples sintered at different temperatures and time are 89.12% (3 h, 1550 °C), 94.37% (6 h, 1550 °C), 95.50% (12 h, 1550 °C), and 96.91% (2.5 h, 1600 °C), respectively. It has been shown that high temperature process resulted in relatively higher sintered densities with a more uniform packing behavior. For maximized density of sintered $La_{10}(SiO_4)_6O_3$ pellet, sufficient sintering temperatures using solid state reaction process is preferred. Plane view SEM images of the sintered samples are shown in Fig. 5. The grain sizes increased on average of 1.0–μm as the sintering temperature and sintering time increased from 1550 °C/3 h to 1550 °C/6 h, 1550 °C/12 h and 1600 °C/2.5 h. It is also evident that the porosity of 1600 °C-sintered sample corresponded to a high sintered density is 2.1% at a bulk density of 5.441 g cm^{-3}.

In order to realize the benefits of thermal pretreatment process applied to the as-purchased La_2O_3 powder for the further preparation of $La_{10}(SiO_4)_6O_3$ pellets, the calcined p-La_2O_3/SiO_2 and t-La_2O_3/SiO_2 mixtures forming into $La_{10}(SiO_4)_6O_3$ powder with and without secondary phases were uniaxially pressed into the $La_{10}(SiO_4)_6O_3$ pellets and then sintered at 1600 °C for 2.5 h in air. Fig. 6 showed the Arrhenius plot of the conductivities of these two kinds of $La_{10}(SiO_4)_6O_3$ pellets determined by two-probe DC method. The existence of secondary phases in $La_{10}(SiO_4)_6O_3$ pellet resulted in a lower conductivity than that of pure $La_{10}(SiO_4)_6O_3$ pellet. The activation energies (Ea) for these two $La_{10}(SiO_4)_6O_3$ samples are also obtained and listed in Fig. 6. Ea values of 0.81 eV for pure $La_{10}(SiO_4)_6O_3$ pellet were larger than the previous reports [10–13], but apparently lower than that of $La_{10}(SiO_4)_6O_3$ pellet with secondary phases (0.86 eV). From the results of materials characterization and conductivity measurement, thermal pretreatment process applied to the as-purchased La_2O_3 powder for the further preparation of $La_{10}(SiO_4)_6O_3$ pellets could effectively eliminate the formation of secondary phases during the calcination or sintering process. Furthermore, for the application of SOFC, the requirement for the ionic conductivity of electrolytes at the operation temperature of 700 °C is 10^{-2} S/cm [16–18]. In Fig. 6, the conductivities of pure $La_{10}(SiO_4)_6O_3$ pellet at 700 °C is 1.1×10^{-3} S/cm, which is subpar to the common SOFC electrolyte material i.e., 8YSZ. Thus, the additional ion doping into the Si-site or La-site was believed to effectively enhance the conductivity of $La_{10}(SiO_4)_6O_3$ samples as the electrolytes for SOFC use [19–23].

For practical application of SOFC electrolyte, the material should be thermochemically stable in reducing atmosphere (H_2 or CH_4 gas) and high temperature conductions without any degradation. Eight-hour reduction-resistant stability tests of bulk samples under 20% H_2 reducing atmosphere in TGA chamber were performed in this study. Fig. 7 shows the weight changes of $La_{10}(SiO_4)_6O_3$ pellets under 20% H_2 reducing atmosphere at 500–800 °C, which represented superior thermochemical stability without any apparent weight loss. From the XRD analyses in Fig. 8, no metallic species, no secondary phases, and no apparent peak shift in pure $La_{10}(SiO_4)_6O_3$ pellet were observed after 8-h reduction-resistant stability tests at 500–800 °C.

Common electrolytes of Bi_2O_3, GDC10 and 8YSZ were also used for the comparison of thermochemical stability under 20% H_2 reducing atmosphere in TGA chamber. So far, δ-cubic Bi_2O_3 is well known for its exceptional ionic conductivity of oxygen ions, but the problems of using Bi_2O_3 as SOFC electrolyte currently encounter the low chemical stability in reducing atmospheres and narrow phase stability temperature range. According to the theoretical calculation, the theoretical maximum oxygen capacity of Bi_2O_3 which means the total weight loss after the complete reduction is 10.3%. An obvious weight loss of 8.2% after 3 h reduction-resistant stability tests shown in Fig. 9, indicating most of Bi_2O_3 was reduced or reacted by H_2 gas to form metallic bismuth (Bi) electronic conductors, which is not applicable for SOFC. Therefore, through suitable doping some aliovalent species, the high ionic

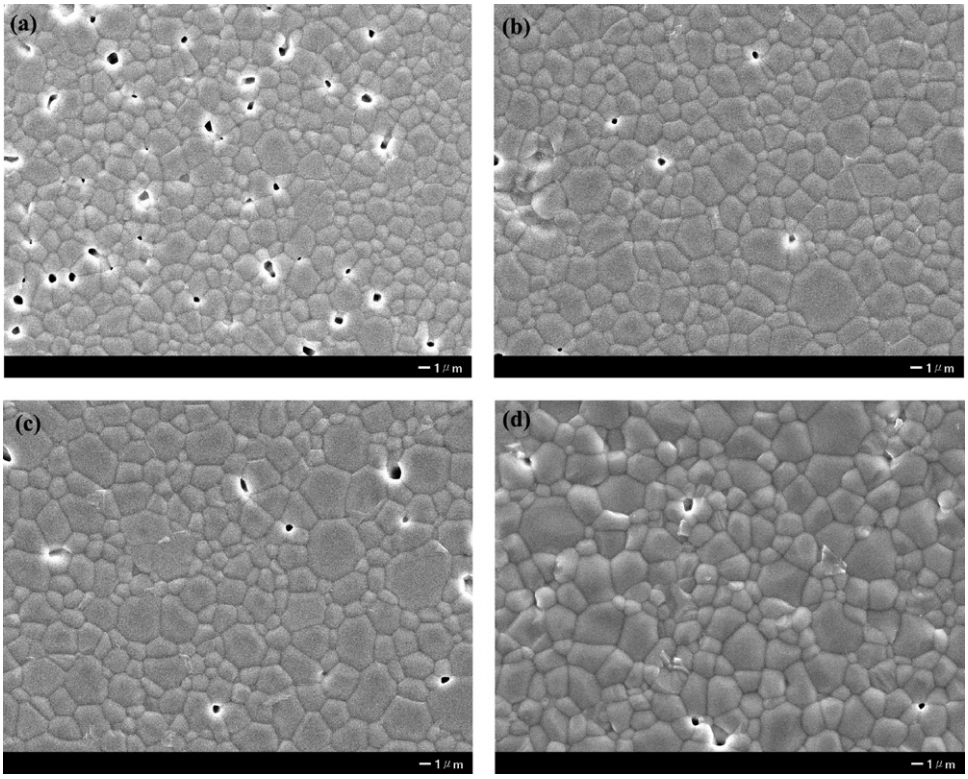

Fig. 5. SEM surface morphology of $La_{10}(SiO_4)_6O_3$ pellets sintered at (a) 1550 °C for 3 h, (b) 1550 °C for 6 h, (c) 1550 °C for 12 h, and (d) 1600 °C for 2.5 h.

conduction phase is believed to be stabilized [5,24,25]. Our previous study also found that 14.3 mol% TiO_2 doped in Bi_2O_3 ($Bi_{12}TiO_{20}$) after reduction-resistant stability tests by TGA revealed possible upper application temperature is below 700 °C under CH_4 atmosphere [26].

Pure stoichiometric CeO_2 has the calcium fluoride (fluorite) type of structure and is known to be an electrical conductor. However when ceria is doped with oxides of divalent or trivalent metals, the ionic conductivity becomes much larger than the electronic conductivity [27]. According to the comparison of the ionic conductivities of oxide doped ceria by Steele, the most appropriate composition for IT-SOFC at 500 °C is $Ce_{0.9}Gd_{0.1}O_{1.95}$ (GDC10) [8,17]. From the reduction-resistant stability tests of GDC10, the small weight loss of 1.1% might be due to the chemical reaction of the lattice oxygen of GDC10 with hydrogen gas, which subsequently resulted in the partial reduction of Ce^{4+} to Ce^{3+} states. The associated electronic conductivity from the Ce^{3+} states in GDC10 can produce an internal short circuit in the SOFC stack, which can significantly lower the efficiency and performance of the SOFC [17]. Due to the apparent weight losses by the reduction of Bi_2O_3 and GDC10 under reducing atmosphere, this problem can be solved by using an additional ultra-thin interfacial electrolyte layer (YSZ) which prevents the electronic transport [28].

8YSZ as the electrolytes have been favored several decades in traditional SOFCs system operated at high temperatures (above 1000 °C) because of its pure ionic conductor and chemical stability in reducing atmosphere at the elevated temperature. As done by reduction-resistant stability tests, 8YSZ represents superior thermochemical stability under H_2 gas without any weight loss. Due to its low ionic conductivity, however, SOFCs systems using 8YSZ as electrolyte usually operated at elevated temperatures (800–1000 °C) for a higher efficiency of power generators. For the application of intermediate temperature SOFCs (500–700 °C), a thin-film 8YSZ electrolyte (<10 μm) maintaining the higher power generation efficiency was discussed elsewhere [29,30].

The single phase $La_{10}(SiO_4)_6O_3$ with an apatite structure prepared in this study shows a good thermochemical stability as the same as 8YSZ. According to the report by Nakayama and Sakamoto [12] pure lanthanum silicate possessed a pure ionic conduction with a transport number of 1.0 over a wide range of oxygen partial pressure. However, the ionic conductivity of pure $La_{10}(SiO_4)_6O_3$ is not high enough (1.1×10^{-3} S/cm at 700 °C shown in Fig. 6), two models of cation doping in this apatite-type structure are addressed. Divalent (Sr^{2+}, $r = 1.20$ Å) or trivalent (Nd^{3+}, $r = 1.09$ Å) ions with the comparable ionic radii to La^{3+} ($r = 1.10$ Å) are proposed to occupy the La site, which resulted in an increase of the conductivity [19,20]. Smaller cation such as Al^{3+} or Ga^{3+} doping of the Si lattice was also reported to enhance the ionic conductivity [21–23]. Therefore it was believed that cation doping in this apatite-type $La_{10}(SiO_4)_6O_3$ is a promising candidate as the solid electrolytes for IT-SOFCs because of its high ionic conductivity and excellent thermochemical stability under reducing atmosphere.

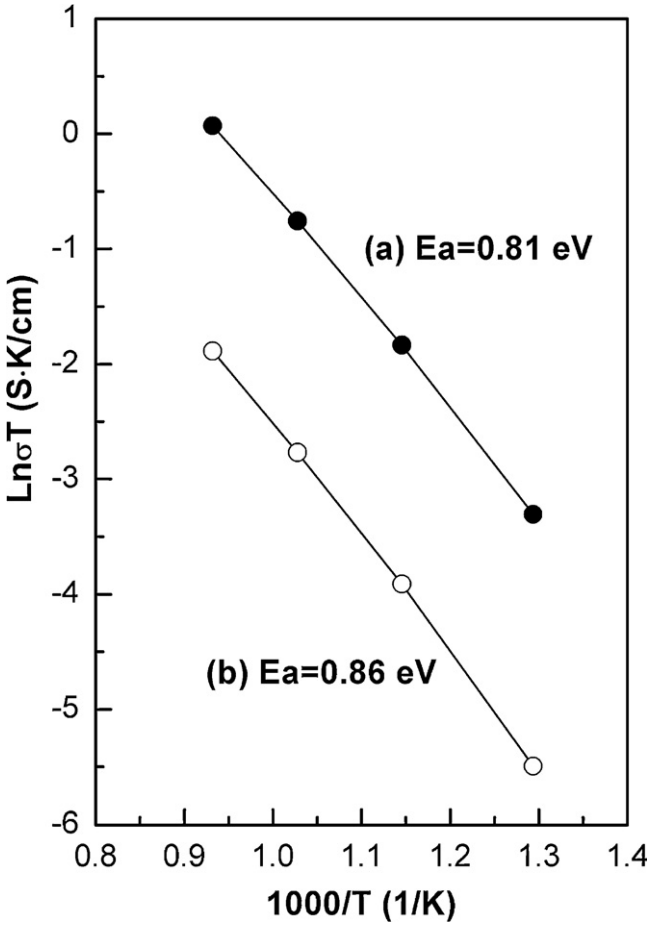

Fig. 6. Arrhenius plot of the conductivity as a function of temperatures for 1600 °C-sintered pellets (a) pure $La_{10}(SiO_4)_6O_3$ and (b) $La_{10}(SiO_4)_6O_3$ with secondary phases.

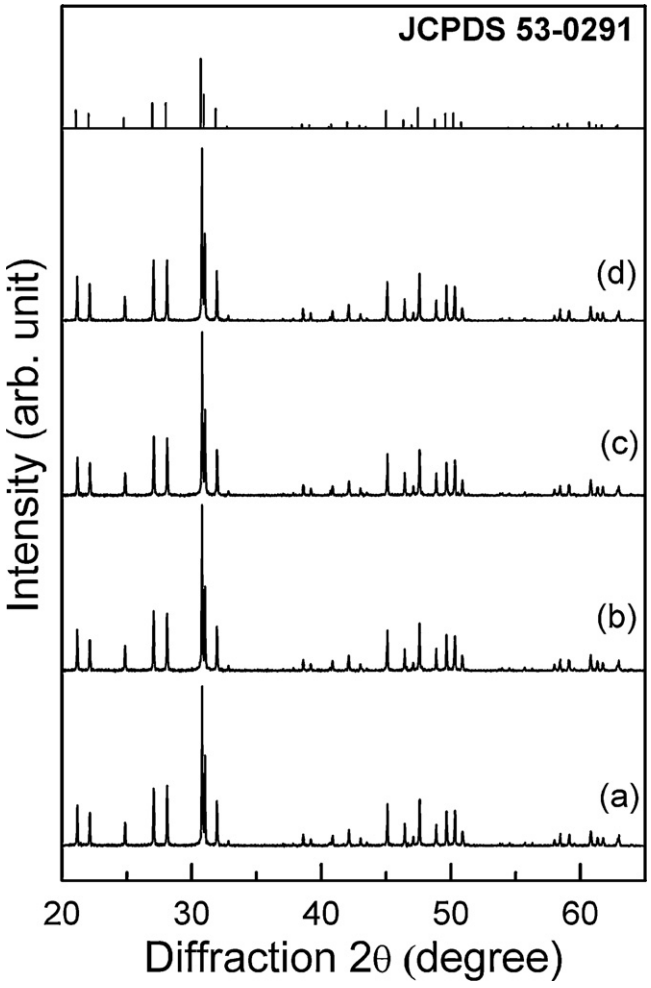

Fig. 8. XRD spectra of pure $La_{10}(SiO_4)_6O_3$ pellets after 8-h reduction-resistant stability tests under various reaction temperatures (a) 500 °C, (b) 600 °C, (c) 700 °C, and (d) 800 °C.

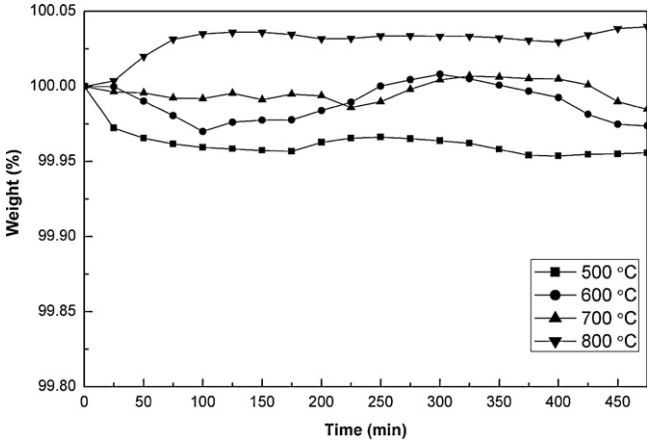

Fig. 7. Eight-hour reduction-resistant stability tests of pure $La_{10}(SiO_4)_6O_3$ pellets under various reaction temperatures (a) 500 °C, (b) 600 °C, (c) 700 °C, and (d) 800 °C.

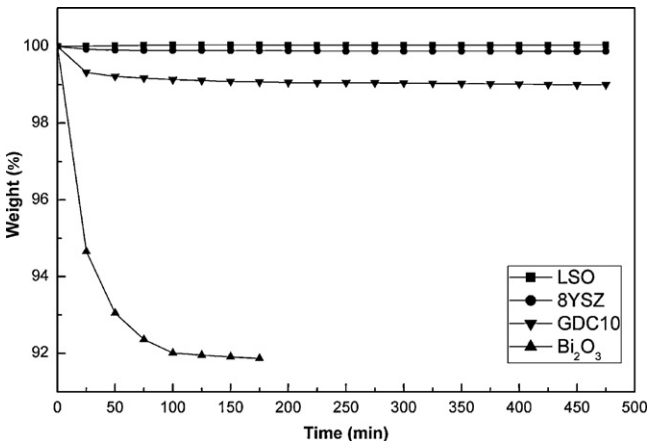

Fig. 9. Comparison of 8YSZ, Bi_2O_3 and GDC10 and $La_{10}(SiO_4)_6O_3$ pellets after reduction-resistant stability tests.

4. Conclusions

Pure $La_{10}(SiO_4)_6O_3$ powder with an apatite phase was prepared through a suitable thermal pretreatment of as-purchased La_2O_3 powder at 1000 °C for 5 h, well-mixed with SiO_2 by high energy ball milling, and subsequently calcined at 1200 °C for 10 h. The high relative sintered density of 96.91% was obtained at 1600 °C for 2.5 h. The higher conductivity of pure $La_{10}(SiO_4)_6O_3$ sintered pellet with an activation energy of 0.81 eV from the conductivity measurement, implying the existence of secondary phases inside $La_{10}(SiO_4)_6O_3$ behaved as a blocking effect of ionic conduction through the electrolytes. The secondary phases inside $La_{10}(SiO_4)_6O_3$ could be recognized as the higher resistance of ionic conduction. In addition, pure $La_{10}(SiO_4)_6O_3$ after 8-h reduction-resistant stability tests under 20% H_2 reducing atmosphere at 500–800 °C represented the behavior of a good thermochemical stability without any sign of phase separation or reduction, as compared to the well-developed YSZ electrolyte.

Acknowledgment

The authors would like to thank the National Science Council of the Republic of China for financially supporting this research under contract no. NSC 99-2221-E-011-044.

References

[1] V.V. Kharton, F.M.B. Marques, A. Atkinson, Transport properties of solid oxide electrolyte ceramics: a brief review, Solid State Ionics 174 (2004) 135–149.
[2] H. Huang, M. Nakamura, P. Su, R. Fasching, Y. Saito, F.B. Prinz, High-performance ultrathin solid oxide fuel cells for low temperature operation, J. Electrochem. Soc. 154 (2007) B20–B24.
[3] Y.L. Kuo, C. Lee, Y.S. Chen, H. Liang, Gadolinia-doped ceria films deposited by RF reactive magnetron sputtering, Solid State Ionics 180 (2009) 1421–1428.
[4] M. Pan, G.Y. Meng, H.W. Xin, C.S. Chen, D.K. Peng, Y.S. Lin, Pure and doped CeO_2 thin films prepared by MOCVD process, Thin Solid Films 324 (1998) 89–93.
[5] C.H. Weng, W.C.J. Wei, Synthesis and properties of homogeneous Nb-doped bismuth oxide, J. Am. Ceram. Soc. 93 (2010) 3124–3129.
[6] Y. Higuchi, M. Sugawara, K. Hosoi, M. Sakamoto, S. Nakayama, Oxide ionic conductivities of apatite-type lanthanum silicates and germanates and their possibilities as an electrolyte of lower temperature operating SOFC, Ceram. Int. 36 (2010) 955–959.
[7] B.C.H. Steele, Appraisal of $Ce_{1-y}Gd_yO_{2-y/2}$ electrolytes for IT-SOFC operation at 500 °C, Solid State Ionics 129 (2000) 95–110.
[8] J.M. Porras-Vázquez, E.R. Losilla, L. León-Reina, D. Marrero-López, M.A.G. Aranda, Microstructure and oxide ion conductivity in a dense $La_{9.33}(SiO_4)_6O_2$ oxy-apatite, J. Am. Ceram. Soc. 92 (2009) 1062–1068.
[9] R. Ali, M. Yashima, Y. Matsushita, H. Yoshioka, K. Ohoyama, F. Izumi, Diffusion path of oxide ions in an apatite-type oonic conductor $La_{9.69}(Si_{5.70}Mg_{0.30})O_{26.24}$, Chem. Mater. 20 (2008) 5203–5208.
[10] H. Yoshioka, Y. Nojiri, Tanase, Ionic conductivity and fuel cell properties of apatite-type lanthanum silicates doped with Mg and containing excess oxide ions, Solid State Ionics 179 (2008) 2165–2169.
[11] S. Nakayama, T. Kageyama, H. Aono, Y. Sadaoka, Ionic conductivity of lanthanoid silicates, $Ln_{10}(SiO_4)_6O_3$ (Ln = La, Nd, Sm, Gd, Dy, Y, Ho, Er and Yb), J. Mater. Chem. 5 (1995) 1801–1805.
[12] S. Nakayama, M. Sakamoto, Electrical properties of new type high oxide ionic conductor $RE_{10}Si_6O_{27}$ (RE = La, Pr, Nd, Sm, Gd, Dy), J. Eur. Ceram. Soc. 18 (1998) 1413–1418.
[13] E. Béchade, I. Julien, T. Iwata, O. Masson, P. Thomas, E. Champion, K. Fukuda, Synthesis of lanthanum silicate oxyapatite materials as a solid oxide fuel cell electrolyte, J. Eur. Ceram. Soc. 28 (2008) 2717–2724.
[14] T. Nakao, A. Mineshige, M. Kobune, T. Yazawa, H. Yoshioka, Chemical stability of $La_{10}Si_6O_{27}$ and its application to electrolytes for solid oxide fuel cells, Solid State Ionics 179 (2008) 1567–1569.
[15] S. Célérier, C. Laberty, F. Ansart, P. Lenormand, P. Stevens, New chemical route based on sol–gel process for the synthesis of oxyapatite $La_{9.33}Si_6O_{26}$, Ceram. Int. 32 (2006) 271–276.
[16] N. Oishi, A. Atkinson, N.P. Brandon, J.A. Kilner, B.C.H. Steele, Fabrication of an anode-supported gadolinium-doped ceria solid oxide fuel cell and its operation at 550 °C, J. Am. Ceram. Soc. 88 (2005) 1394–1396.
[17] B.C.H. Steele, A. Heinzel, Materials for fuel-cell technologies, Nature 414 (2001) 345–352.
[18] D.J.L. Brett, A. Atkinson, D. Cumming, E. Ramírez-Cabrera, R. Rudkin, N.P. Brandon, Methanol as a direct fuel in intermediate temperature (500–600 °C) solid oxide fuel cells with copper based anodes, Chem. Eng. Sci. 60 (2005) 5649–5662.
[19] H. Arikawa, H. Nishiguchi, T. Ishihara, Y. Takita, Oxide ion conductivity in Sr-doped $La_{10}Ge_6O_{27}$ apatite oxide, Solid State Ionics 136–137 (2000) 31–37.
[20] R.D. Shannon, C.T. Prewitt, Effective ionic radii in oxides and fluorides, Acta Cryst. B25 (1969) 925–946.
[21] J.E.H. Sansom, J.R. Tolchard, P.R. Slater, M.S. Islam, Synthesis and structural characterisation of the apatite-type phases $La_{10-x}Si_6O_{26+z}$ doped with Ga, Solid State Ionics 167 (2004) 17–22.
[22] A. Najib, J.E.H. Sansom, J.R. Tolchard, P.R. Slater, M.S. Islam, Doping strategies to optimise the oxide ion conductivity in apatite-type ionic conductors, Dalton Trans. 19 (2004) 3106–3109.
[23] I. Santacruz, J.M. Porras-Vázquez, E.R. Losilla, M.I. Nieto, M.A.G. Aranda, Colloidal processing and characterization of aluminum-doped lanthanum oxyapatite, $La_{10}AlSi_5O_{26.5}$, J. Am. Ceram. Soc. 94 (2011) 117–123.
[24] H. Iwahara, T. Esaka, T. Sato, T. Takahashi, Formation of high oxide ion conductive phases in the sintered oxides of the system Bi_2O_3–Ln_2O_3 (Ln = La–Yb), J. Solid State Chem. 39 (1981) 173–180.
[25] N. Jiang, E.D. Wachsman, Structural stability and conductivity of phase-stabilized cubic bismuth oxides, J. Am. Ceram. Soc. 82 (1999) 3057–3064.
[26] Y.L. Kuo, L.D. Liu, S.E. Lin, C.H. Chou, W.C.J. Wei, Assessment of structurally stable cubic $Bi_{12}TiO_{20}$ as intermediate temperature solid oxide fuels electrolyte, J. Eur. Ceram. Soc. 31 (2011) 3119–3125.
[27] M. Mogensen, N.M. Sammes, G.A. Tompsett, Physical, chemical and electrochemical properties of pure and doped ceria, Solid State Ionics 129 (2000) 63–94.
[28] K.Z. Fung, H.D. Baek, A.V. Virkar, Thermodynamic and kinetic considerations for Bi_2O_3-based electrolytes, Solid State Ionics 52 (1992) 199–211.
[29] P. Briois, A.A. Billard, A comparison of electrical properties of sputter-deposited electrolyte coatings dedicated to intermediate temperature solid oxide fuel cells, Surf. Coat. Technol. 201 (2006) 1328–1334.
[30] P. Coddet, M.C. Pera, A. Billard, Reactive co-sputter deposition of YSZ coatings using plasma emission monitoring, Surf. Coat. Technol. 205 (2011) 3987–3991.